Supporting Information:

Expanding the Hole Delocalization Range in Excited Molecules for Stable Organic Light-Emitting Diodes Employing Thermally Activated Delayed Fluorescence

Xinyuan Zheng,‡[a] Fangyi Cao,‡[a,b] Chao Wang,[c] Taiju Tsuboi,[a] Yunhui Zhu,[a] Qi Ai,[d]

Chao Deng,[a] Dan Wang,*[a] Liwu Su,[a] Zhang Liu,[a] Qisheng Zhang*[a]

[a] MOE Key Laboratory of Macromolecular Synthesis and Functionalization, Department of Polymer Science and Engineering, Zhejiang University, Hangzhou 310027, P. R. China.

[b] Yungu (Gu'an) Technology Co. Ltd., Hebei, 065500, China.

[c] Singapore University of Technology and Design, 8 Somapah Road, 487372, Singapore.

[d] State Key Laboratory Breeding Base of Green Chemistry-Synthesis Technology, College of Chemical Engineering, Zhejiang University of Technology, Hangzhou, 310014, China.

E-mail: qishengzhang@zju.edu.cn; 0016720@zju.edu.cn

‡ These authors contributed equally.

Contents

1. Supplemental Tables and Figures

Table S1. Calculated $E_{VA}(S_1)$ and $E_{VA}(T_1)$ using various exchange-correlation functionals and 6-31G* basis set based on B3LYP optimized geometries, and calculated CT amount (q), optimal HF%, $E_{0-0}(^3LE)$, $E_{0-0}(^1CT)$ and $E_{0-0}(^3CT)$ of the compounds in vacuum.[1]
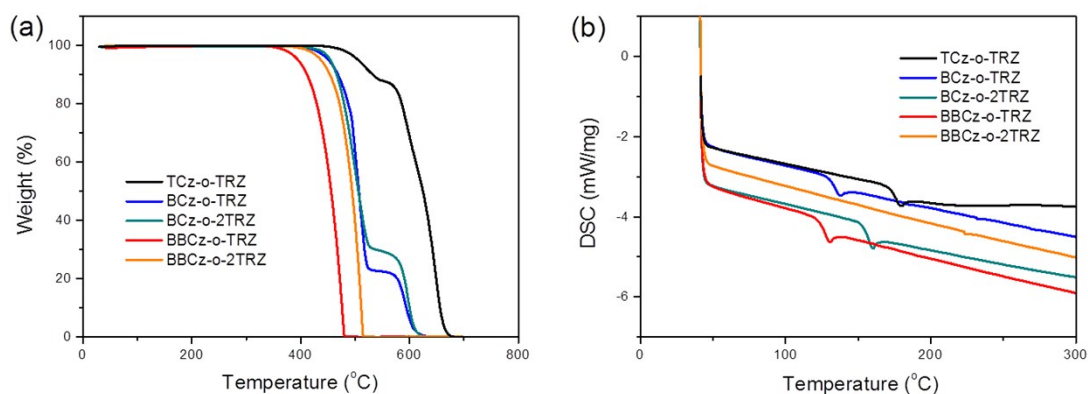
	functional	TCz-o-TRZ	BCz-o-TRZ	BCz-o-2TRZ	BBCz-o-TRZ	BBCz-o-2TRZ
	B3LYP	2.57	2.63	2.62	2.56	2.57
	PBE0	2.77	2.83	2.81	2.75	2.76
$E_{VA}(S_1)$	MPW1B95	2.94	3.00	2.98	2.91	2.93
(eV)	BMK	3.29	3.35	3.33	3.25	3.28
	M06-2X	3.58	3.63	3.61	3.52	3.56
	M06-HF	4.42	4.42	4.41	4.34	4.38
	B3LYP	2.53	2.60	2.58	2.53	2.53
	PBE0	2.71	2.77	2.75	2.67	2.67
$E_{VA}(T_1)$	MPW1B95	2.88	2.94	2.92	2.84	2.84
(eV)	BMK	3.18	3.22	3.21	3.06	3.06
	M06-2X	3.43	3.47	3.45	3.27	3.27
	M06-HF	3.87	3.90	3.90	3.70	3.70
CT amount (e) [a]		0.93	0.94	0.90	0.94	0.91
Optimal HF% [b]		37.4	39.5	37.8	39.5	38.2
$E_{VA}(S_1,OHF)$ (eV) [c]		3.16	3.27	3.20	3.18	3.17
$E_{0-0}(^1CT)$ (eV) [d]		2.92	3.03	2.96	2.94	2.93
$E_{0-0}(^3CT)$ (eV) [e]		2.87	2.99	2.91	2.90	2.89
$E_{0-0}(^3LE)$ (eV) [f]		2.89	2.91	2.91	2.76	2.76
ΔE_{ST} (eV)		0.05	0.12	0.05	0.18	0.16

[a] Orbital compositions were analyzed using Multiwfn.[2] [b] OHF=$42q$.[3] [c] The $E_{VA}(S_1)$ corresponding to the OHF can be read from the best fit straight line for a double log plot of $E_{VA}(S_1)$ against HF%. [d] $E_{0-0}(^1CT) = E_{VA}(S_1, OHF)-0.24eV$.[3] [e] $E_{0-0}(^3CT) = E_{0-0}(S_1, OHF)-[E_{VA}(S_1, B3LYP)-E_{VA}(T_1, B3LYP)]$.[3] [f] $E_{0-0}(^3LE) = E_{VA}(T_1, M06-HF)/1.3-0.09$ eV.[3]
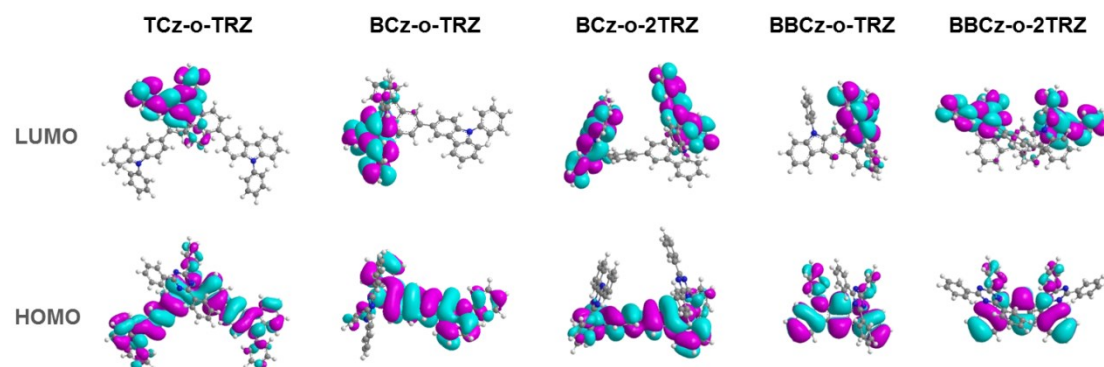

Figure S1. HOMO and LUMO isosurface plots of the S_0 states of the compounds calculated at the B3LYP/6-31G* level.

Figure S2. TGA (a) and DCS (b) curves of the five investigated compounds under nitrogen flow. The 5 wt% weight loss temperatures for TCz-o-TRZ, BCz-o-TRZ, BCz-o-2TRZ, BBCz-o-TRZ and BBCz-o-2TRZ are 505℃，451℃, 454℃, 395℃ and 437℃, respectively. The T_g for TCz-o-TRZ, BCz-o-TRZ, BCz-o-2TRZ and BBCz-o-TRZ are 179℃，137℃, 160℃ and 130℃, respectively.
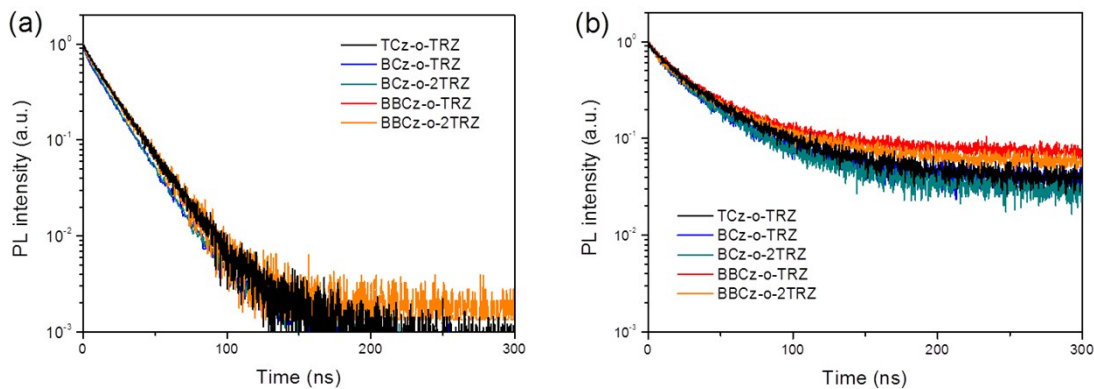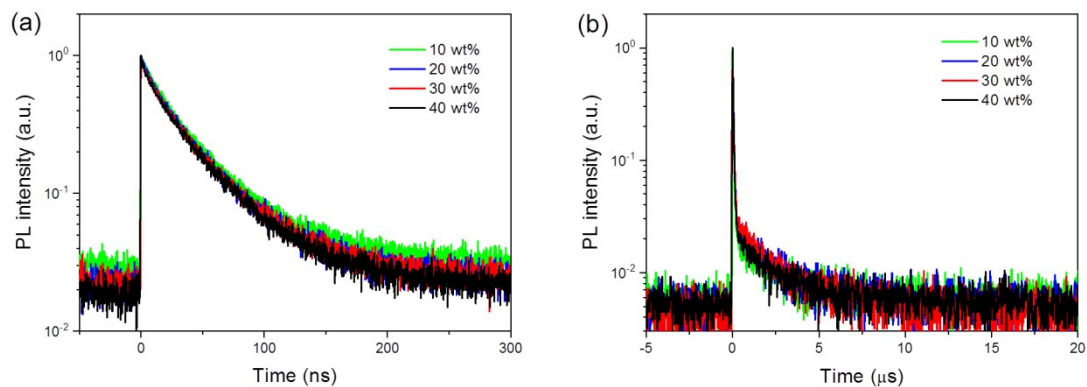

Figure S3. Transient decay spectra of the investigated molecules in oxygen-free toluene (a) and doped PYD2 film (10 wt%) (b) at room temperature.
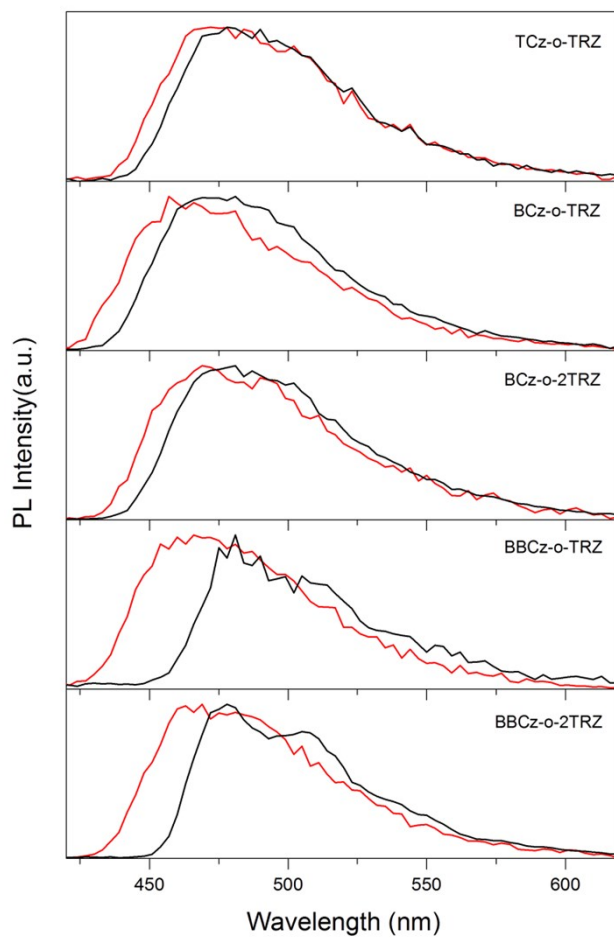
Figure S4. Fluorescence (1 ns component, red line) and phosphorescence (100-1000 μs component, black line) spectra of the investigated molecules in toluene at 77 K.
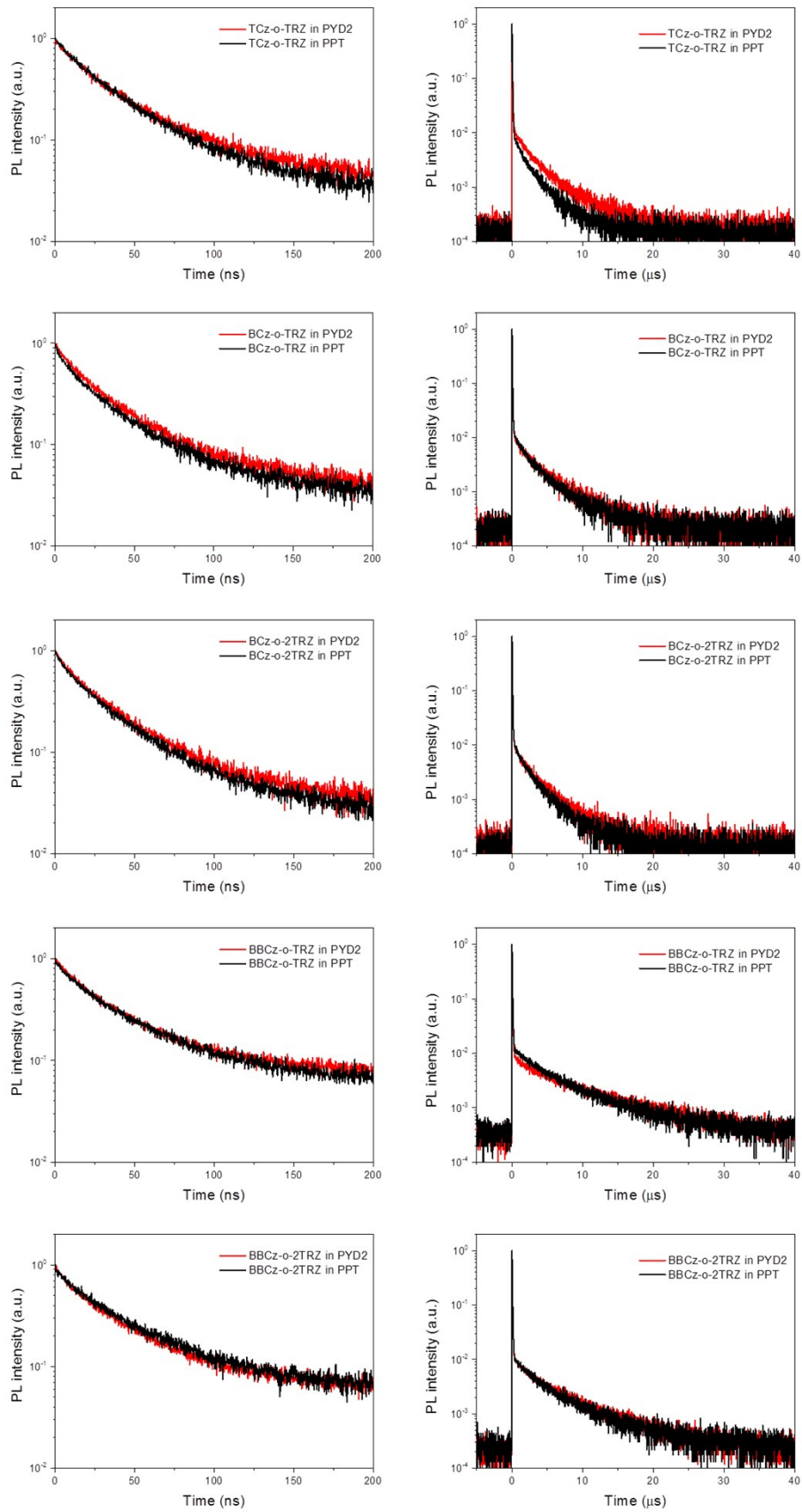
Figure S5. Transient decay spectra of the investigated molecules in doped PYD2 and PPT films (10 wt%) at room temperature.

Figure S6. The doping concentration dependent transient decay spectra of BCz-o-2TRZ doped PYD2 films at room temperature.
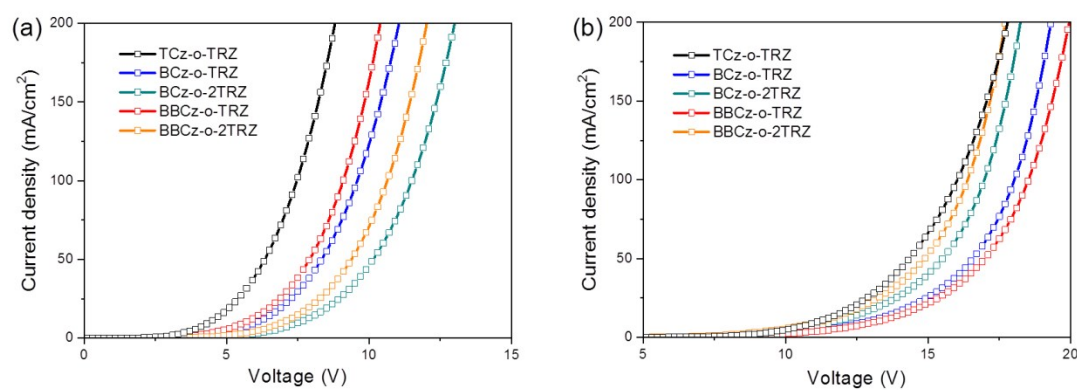
Figure S7. Current density-voltage characteristics of the hole-only devices with a structure of ITO/MoO$_3$ (10 nm)/30 wt% TADF compound: PYD2 (60 nm)/MoO$_3$ (10 nm)/Al (120 nm) (**a**) and the electron-only devices with a structure of ITO/Li$_2$CO$_3$ (2 nm)/30 wt% TADF compound: PYD2 (60 nm)/Li$_2$CO$_3$ (2 nm)/Al (100 nm) (**b**).
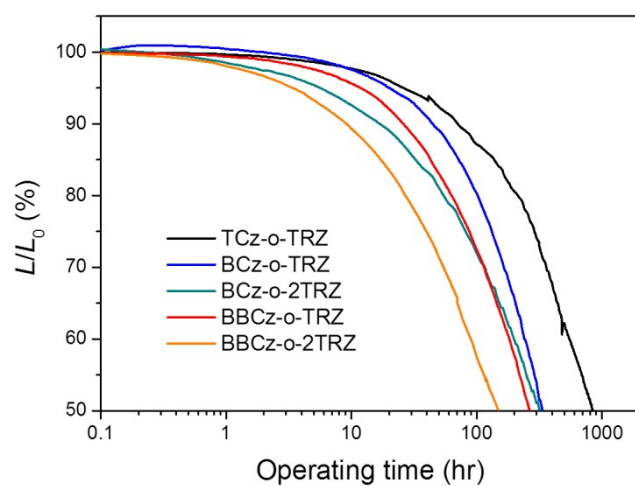
Figure S8. LT50 at a fixed current density with an L_0 of 1000 cd/m^2. The TADF emitters were doped into a PPT host in device structure shown in Figure 3a.
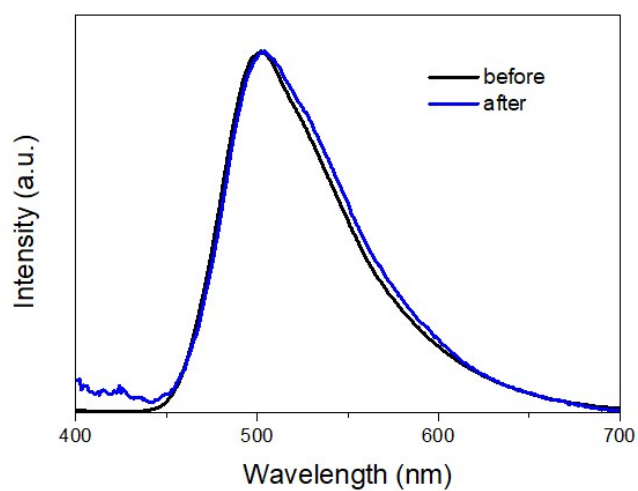
Figure S9. EL spectra before and after 100 hr operation for the device employing BCz-o-2TRZ as emitter and PYD2 as host.
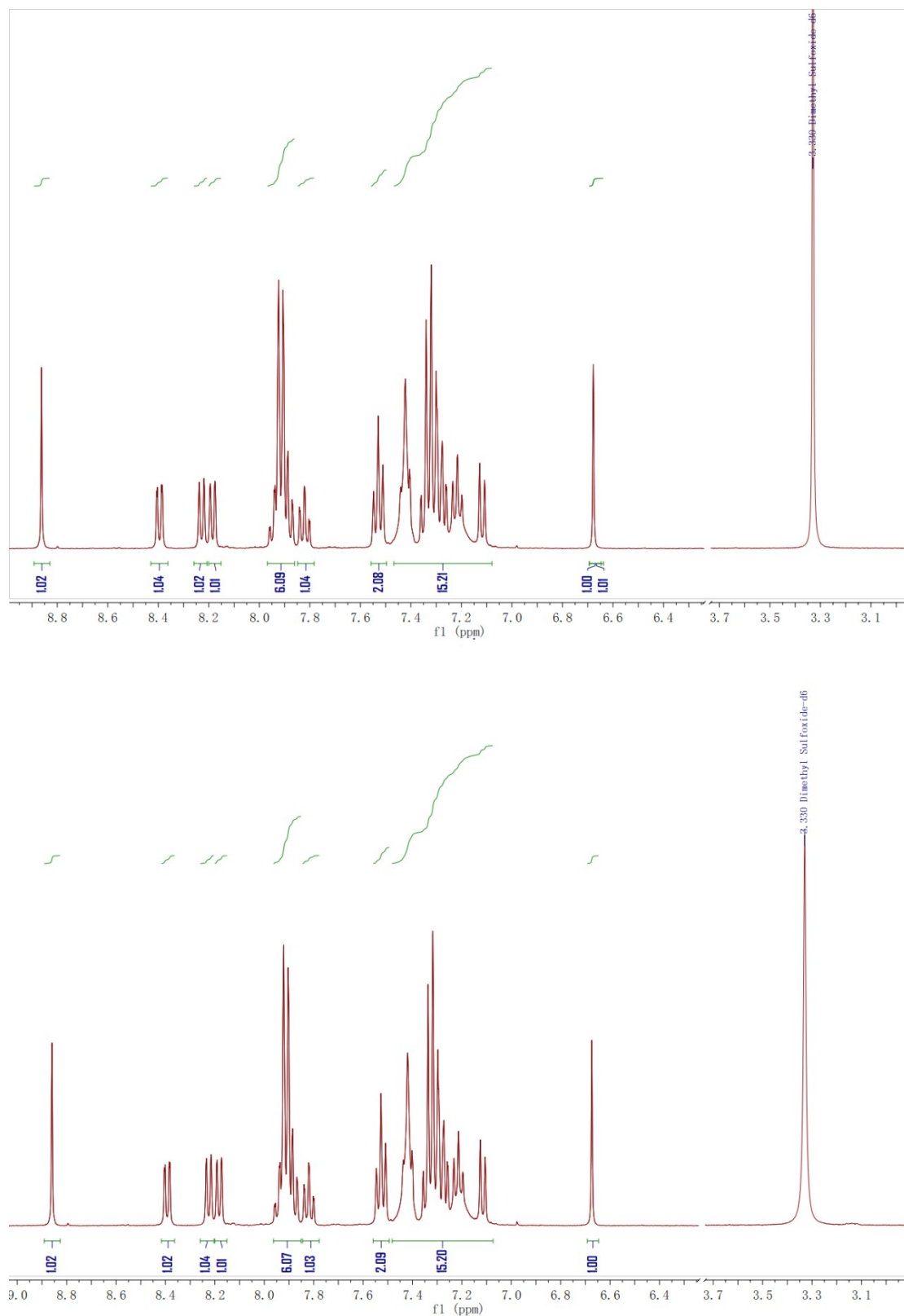
Figure S10. ¹H NMR spectra of BBCz-o-TRZ in DMSO-d6 before (upper image) and after (lower image) 365 nm UV irradiation for 30 min.
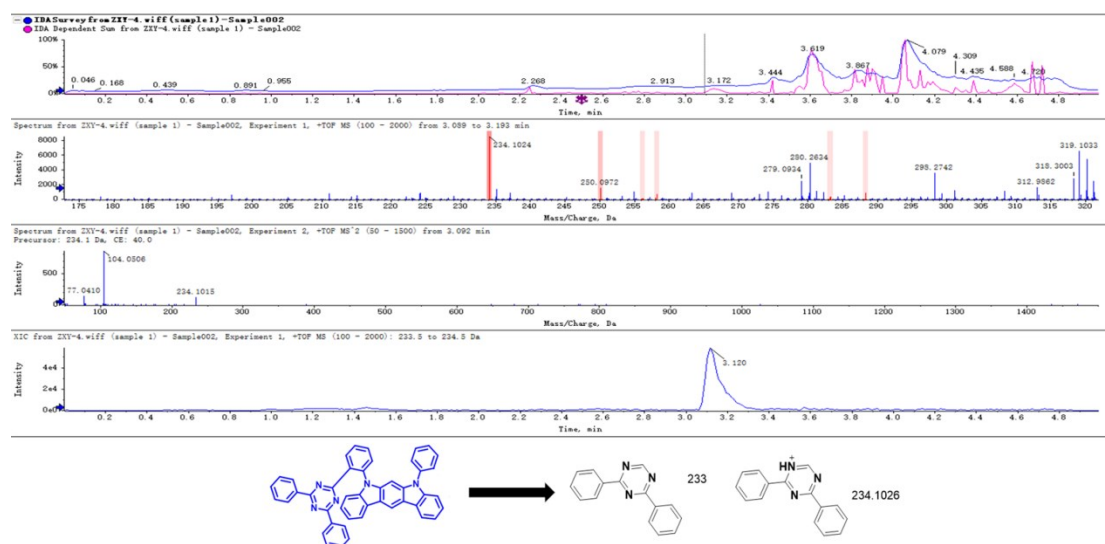
Figure S11. HPLC-MS of BBCz-o-TRZ after 365 nm UV irradiation for 30 min. A component with a molecular weight in the ranges of 233.5−234.5 Da was detected.
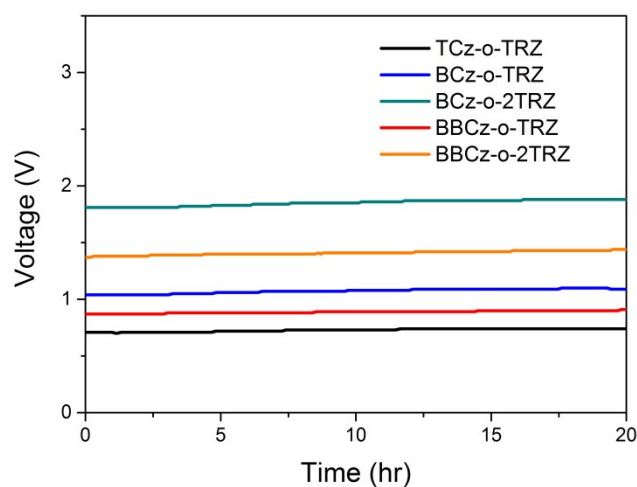
Figure S12. Voltage-operating time characteristics at a fixed current density of 1.0 mA/cm^2 for the hole-only devices with a structure of ITO/MoO$_3$ (10 nm)/TADF compound (60 nm)/MoO$_3$ (10 nm)/Al (120 nm).
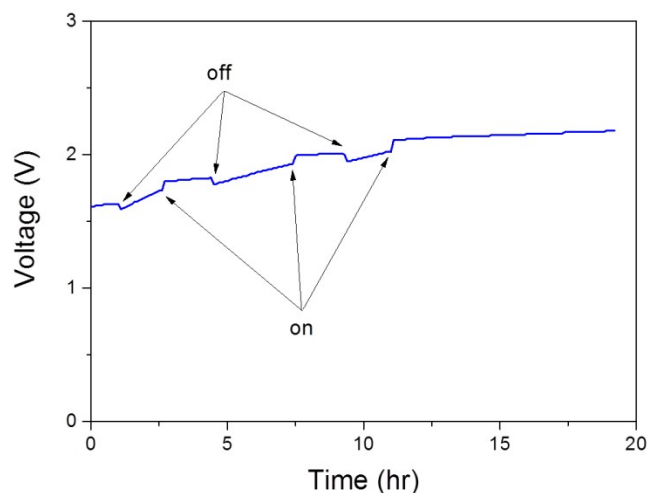
Figure S13. Voltage-operating time characteristics at a fixed current density of 1.0 mA/cm^2 for the hole-only device ITO/MoO$_3$ (10 nm)/BBCz-o-2TRZ (60 nm)/MoO$_3$ (10 nm)/Al (120 nm). A discontinuous 532 nm illumination was applied to the device during the operation.
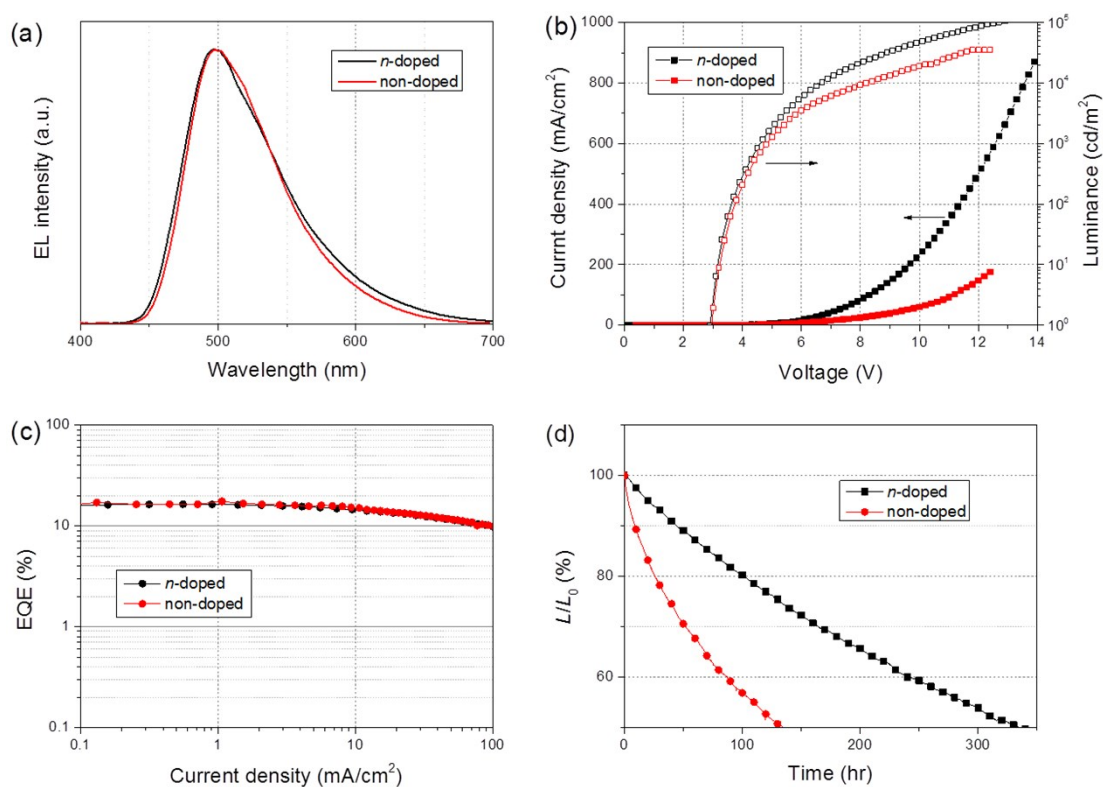
Figure S14. (a) Electroluminescence (EL) spectra at 10 mA/cm^2, (b) luminance-current density-voltage characteristics, (c) EQE-current density characteristics, and (d) luminance-operating time characteristics at fixed current densities (L_0=1000 cd/m^2) of BCz-o-TRZ-based OLEDs with PPT host and a doped (5 wt% Li$_2$CO$_3$: Bepp$_2$) or non-doped (Bepp$_2$) electron-transporting layer.

2. Experimental Section

2.1 Materials and measurement:

All solvents and starting materials were purchased from commercial resources and were used as received unless otherwise stated. The five TADF compounds investigated in this paper were synthesized by the procedures described below and purified by sublimation twice. The OLED materials PYD2, MoO_3, mCP, PPT and Liq were purchased from Jilin Optical and Electronic Materials Co., Ltd. and were used without further purification. Nuclear magnetic resonance spectroscopy (NMR) was recorded on a Bruker Avance III 400 spectrometer (^{1}H: 400 MHz and ^{13}C: 100 MHz) at room temperature using $CDCl_3$ as solvent and tetramethylsilane (TMS) as internal reference. Mass spectra measurements were performed on an IT-TOF (Shimadzu, Japan) in positive ion mode ESI-MS. Accurate mass determination was corrected by calibration using sodium trifluoroacetate clusters as reference. Waters ultra-performance liquid chromatography (Waters Corp., Milford, MA, USA) equipped with a Triple TOF 5600 Plus mass spectrometer (AB SCIEX, Framingham, USA) was used to separate and analyze the degradation products. The UV detector was set at 280 nm.

2.2 Synthesis:
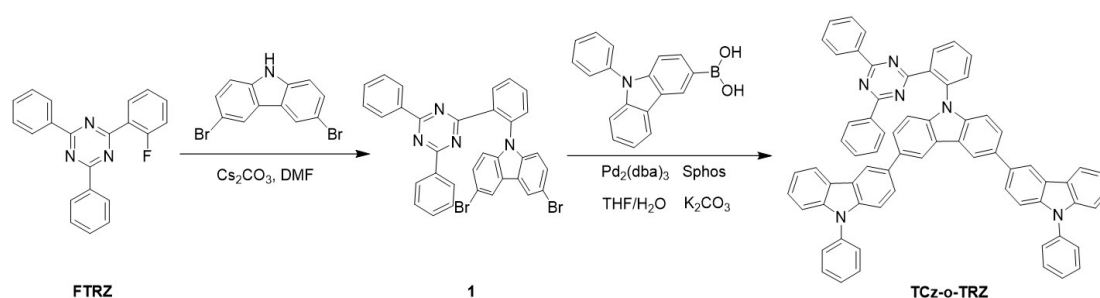
Scheme S1. Synthesis route of TCz-o-TRZ
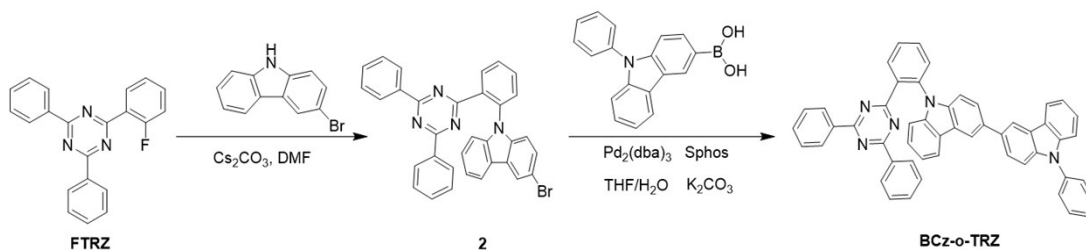
3,6-Dibromo-9-(2-(4,6-diphenyl-1,3,5-triazin-2-yl)phenyl)-9H-carbazole (1):

2-(2-Fluorophenyl)-4,6-diphenyl-1,3,5-triazine (FTRZ) (0.7 g, 2.14 mmol), 3,6-dibromo-9H-carbazole (0.83 g, 2.57 mmol), Cs_2CO_3 (1.39 g, 4.27 mmol) were added

to a 100 ml three-necked flask under argon protection. After the mixture was degassed with argon for 3 times, anhydrous DMF solution (60 mL) was added, and then the mixture was heated to reflux for 24 hours. The reaction was quenched by H_2O. The reaction mixture was cooled to room temperature and extracted with dichloromethane. After the solvent evaporated under a reduced pressure, the residue was purified by column chromatography (DCM/PE=1/20) to afford **1** (1.02 g, 76%). **¹H NMR** (600 MHz, Chloroform-d) δ 8.55 (d, J = 7.8 Hz, 1H), 8.10 (s, 2H), 8.00 (d, J = 7.8 Hz, 4H), 7.95 (d, J = 7.8 Hz, 1H), 7.86 – 7.79 (m, 1H), 7.77 (t, J = 7.5 Hz, 1H), 7.49 (t, J = 7.3 Hz, 2H), 7.39 (dd, J = 8.5, 2.0 Hz, 2H), 7.33 (m, 4H), 7.13 (d, J = 8.6 Hz, 2H).

9'-(2-(4,6-Diphenyl-1,3,5-triazin-2-yl)phenyl)-9,9''-diphenyl-9H,9'H,9''H-3,3':6',3''-tercarbazole (TCz-o-TRZ)

Add **1** (1.02 g, 1.62 mmol), (9-phenyl-9H-carbazol-3-yl)boronic acid (1.16 g, 4.05 mmol), 2-Dicyclohexylphosphino-2',6'-dimethoxybiphenyl (0.079 g, 0.194 mmol), and anhydrous K_2CO_3 (0.67 g, 4.85 mmol) into a 100 ml three-necked flask under argon protection. Tetrahydrofuran (THF, 50 ml) and deionized water (10 ml) was also added to the flask. Tris(dibenzylideneacetone)dipalladium (0.044 g, 0.048 mmol) was added, after the mixture was degassed with argon for 30 minutes, and then the mixture was heated to reflux for 24 hours. The reaction mixture was cooled to room temperature and extracted with dichloromethane. After the solvent evaporated under a reduced pressure, the residue was purified by column chromatography (DCM/PE=1/50) to afford **TCz-o-TRZ** (1.35 g, 90%). **¹H NMR** (400 MHz, CDCl₃) δ 8.64 – 8.56 (m, 1H), 8.45 (t, J = 1.8 Hz, 4H), 8.24 (d, J = 7.7 Hz, 2H), 8.13 – 8.05 (m, 4H), 7.91 – 7.85 (m, 1H), 7.84 – 7.72 (m, 6H), 7.67 – 7.60 (m, 8H), 7.53 – 7.40 (m, 10H), 7.36 – 7.28 (m, 8H). **¹³C NMR** (101 MHz, CDCl₃) δ 172.15, 171.43, 141.67, 141.34, 139.98, 137.83, 136.86, 136.55, 135.56, 134.49, 133.92, 132.84, 132.60, 132.39, 130.75, 129.92, 128.92, 128.36, 127.43, 127.09, 126.19, 124.26, 124.00, 123.63, 120.46, 119.97, 118.92, 109.95, 77.30, 77.04, 76.73. **HRMS** *m/z*: 957.33 [M+H]⁺.
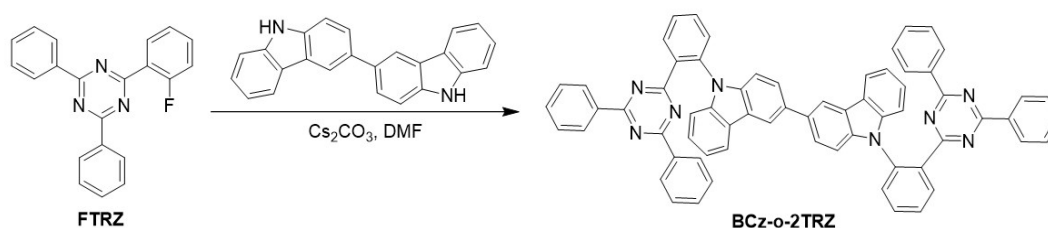
Scheme S2. Synthesis route of BCz-o-TRZ.

3-Bromo-9-(2-(4,6-diphenyl-1,3,5-triazin-2-yl)phenyl)-9H-carbazole (2) :

2-(2-Fluorophenyl)-4,6-diphenyl-1,3,5-triazine (FTRZ) (1.0 g, 3.05 mmol), 3-bromo-9H-carbazole (0.82 g, 3.36 mmol), Cs_2CO_3 (2.5 g, 7.69 mmol) were added to a 100 ml three-necked flask under argon protection. After the mixture was degassed with argon for 3 times, anhydrous DMF solution (60 mL) was added, and then the mixture was heated to reflux for 24 hours. The reaction was quenched by H_2O. The reaction mixture was cooled to room temperature and extracted with dichloromethane. After the solvent evaporated under a reduced pressure, the residue was purified by column chromatography (DCM/PE=1/20) to afford **2** (1.4 g, 83%). **¹H NMR** (400 MHz, CDCl₃) δ 8.55 (d, J = 7.6 Hz, 1H), 8.14 (s, 1H), 8.00 (d, J = 7.6 Hz, 4H), 7.95 (d, J = 7.7 Hz, 1H), 7.82 (t, J = 7.5 Hz, 1H), 7.77 (t, J = 7.5 Hz, 1H), 7.67 (d, J = 7.6 Hz, 1H), 7.48 (t, J = 7.2 Hz, 2H), 7.42 (d, J = 8.6 Hz, 1H), 7.34 (t, J = 7.6 Hz, 5H), 7.20 (t, J = 7.4 Hz, 1H), 7.16 (d, J = 8.2 Hz, 1H), 7.10 (d, J = 8.6 Hz, 1H).

9-(2-(4,6-diphenyl-1,3,5-triazin-2-yl)phenyl)-9'-phenyl-9H,9'H-3,3'-bicarbazole (BCZ-o-TRZ) :

Add **2** (1.4 g, 2.54 mmol), (9-phenyl-9H-carbazol-3-yl)boronic acid (0.87 g, 3.04 mmol), 2-Dicyclohexylphosphino-2',6'-dimethoxybiphenyl (0.125 g, 0.305 mmol), anhydrous K_2CO_3 (1.0 g, 7.24 mmol) into a 100 ml three-necked flask under argon protection. THF (50 ml) and Deionized water (10 ml) was also added to the flask. Tris(dibenzylideneacetone)dipalladium (0.07 g, 0.076 mmol) was added, after the mixture was degassed with argon for 30 minutes, and then the mixture was heated to reflux for 24 hours. The reaction mixture was cooled to room temperature and

extracted with dichloromethane. After the solvent evaporated under a reduced pressure, the residue was purified by column chromatography (DCM/PE=1/50) to afford **BCz-o-TRZ** (1.45 g, 80%). **¹H NMR** (400 MHz, CDCl₃) δ 8.57 (dd, J = 7.7, 1.5 Hz, 1H), 8.43 (d, J = 1.3 Hz, 1H), 8.36 (d, J = 1.3 Hz, 1H), 8.23 (d, J = 7.7 Hz, 1H), 8.10 (d, J = 7.6 Hz, 1H), 8.07 – 8.00 (m, 4H), 7.86 (td, J = 7.5, 1.7 Hz, 1H), 7.77 (tdd, J = 9.4, 8.1, 1.6 Hz, 4H), 7.67 – 7.60 (m, 4H), 7.53 – 7.40 (m, 6H), 7.32 (ddd, J = 7.5, 6.9, 5.0 Hz, 7H), 7.24 – 7.16 (m, 2H). **¹³C NMR** (101 MHz, CDCl₃) δ 172.11, 171.34, 142.24, 141.27, 139.97, 137.81, 136.81, 135.50, 134.54, 133.89, 132.81, 132.57, 132.36, 130.69, 129.92, 128.85, 128.35, 127.44, 127.09, 126.05, 125.83, 124.03, 123.60, 120.39 ,119.97, 119.57, 118.87, 110.20, 109.62, 77.30, 77.04, 76.72. **HRMS** m/z: 716.22 [M+H]⁺.
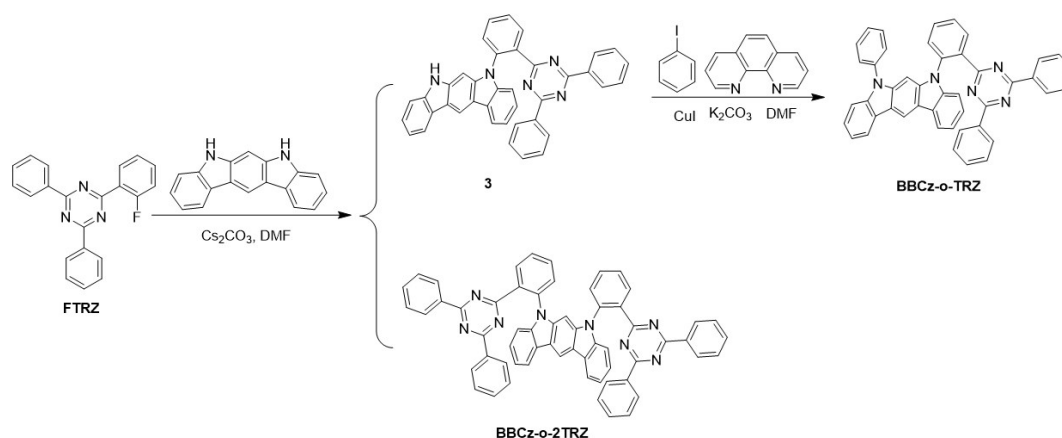

Scheme S3. Synthesis route of BCz-o-2TRZ.

9,9'-Bis(2-(4,6-diphenyl-1,3,5-triazin-2-yl)phenyl)-9H,9'H-3,3'-bicarbazole (BCz-o-2TRZ):

2-(2-Fluorophenyl)-4,6-diphenyl-1,3,5-triazine (FTRZ) (1.59 g, 4.88 mmol), 9H,9'H-3,3'-bicarbazole (0.74 g, 2.22 mmol), Cs₂CO₃ (3.6 g, 11.07 mmol) were added to a 100 ml three-necked flask under argon protection. After the mixture was degassed with argon for 3 times, anhydrous DMF solution (60 mL) was added, and then the mixture was heated to reflux for 24 hours. The reaction was quenched by H₂O. The reaction mixture was cooled to room temperature and extracted with dichloromethane. After the solvent evaporated under a reduced pressure, the residue was purified by column chromatography (DCM/PE=1/20) to afford **BCz-o-2TRZ** (1.57 g, 75%). **¹H NMR** (400 MHz, CDCl₃) δ 8.57 (dd, J = 7.6, 1.5 Hz, 2H), 8.33 (t, J = 1.7 Hz, 2H), 8.09 (d, J = 7.7 Hz, 2H), 8.07 – 8.00 (m, 8H), 7.85 (td, J = 7.5, 1.4 Hz, 2H), 7.78 (ddd,

J = 7.5, 6.0, 2.2 Hz, 4H), 7.72 (dd, J = 8.5, 1.5 Hz, 2H), 7.40 (td, J = 7.3, 1.3 Hz, 4H), 7.35 (dd, J = 8.6, 1.9 Hz, 2H), 7.30 (t, J = 7.6 Hz, 10H), 7.23 − 7.17 (m, 4H). **^{13}C NMR** (101 MHz, CDCl$_3$) δ 172.13, 171.35, 142.20, 141.13, 136.82, 136.35, 135.50, 134.09, 132.80, 132.57, 132.37, 130.69, 128.84, 128.35, 125.96, 124.08, 123.62, 120.35, 119.56, 118.87, 109.93, 109.60, 77.56, 77.03, 76.75. **HRMS** *m*/*z*: 947.31 [M+H]$^+$.

Scheme S4. Synthesis route of BBCz-o-TRZ and BBCz-o-2TRZ.

5-(2-(4,6-Diphenyl-1,3,5-triazin-2-yl)phenyl)-5,7-dihydroindolo[2,3-b]carbazole (3):

2-(2-Fluorophenyl)-4,6-diphenyl-1,3,5-triazine (FTRZ) (1.15 g, 3.5 mmol), 5,7-dihydroindolo[2,3-b]carbazole (1.0 g, 3.9 mmol), Cs$_2$CO$_3$ (2.28 g, 7 mmol) were added to a 100 ml three-necked flask under argon protection. After the mixture was degassed with argon for 3 times, anhydrous DMF solution (60 mL) was added, and then the mixture was heated to reflux for 24 hours. The reaction was quenched by H$_2$O. The reaction mixture was cooled to room temperature and extracted with dichloromethane. After the solvent evaporated under a reduced pressure, the residue was purified by column chromatography (DCM/PE=1/10) to afford **3** (0.77 g, 39%). **^{1}H NMR** (400 MHz, CDCl$_3$) δ 8.65 (s, 1H), 8.58 (dd, J = 7.6, 1.5 Hz, 1H), 8.15 − 8.09 (m, 2H), 7.99 − 7.94 (m, 4H), 7.88 − 7.74 (m, 4H), 7.40 (t, J = 7.4 Hz, 2H), 7.31 (ddd, J = 15.3, 8.2, 1.1 Hz, 4H), 7.26 − 7.16 (m, 8H), 7.07 (s, 1H).

5-(2-(4,6-Diphenyl-1,3,5-triazin-2-yl)phenyl)-7-phenyl-5,7-dihydroindolo[2,3-b]carbazole (BBCz-o-TRZ):

Add **3** (0.77 g, 1.36 mmol), 1,10-phenanthroline (0.015 g, 0.081 mmol), anhydrous K_2CO_3 (0.56 g, 4.08 mmol), CuI (0.16 g, 0.816 mmol) into a 100 ml three-necked flask under argon protection. Anhydrous DMF solution (60 mL) was also added to the flask. Iodobenzene (0.361 g/ 0.20 ml, 1.77 mmol) was added, after the mixture was degassed with argon for 30 minutes, and then the mixture was heated to reflux for 24 hours. The reaction was quenched by H_2O. The reaction mixture was cooled to room temperature and extracted with dichloromethane. After the solvent evaporated under a reduced pressure, the residue was purified by column chromatography (DCM/PE=1/50) to afford **BBCz-o-TRZ** (1.45 g, 80%). **¹H NMR** (400 MHz, $CDCl_3$) δ 8.65 (d, J = 0.6 Hz, 1H), 8.44 (dd, J = 7.7, 1.4 Hz, 1H), 8.15 (dd, J = 12.2, 4.7 Hz, 2H), 8.03 – 7.97 (m, 4H), 7.77 (ddd, J = 14.9, 7.4, 1.4 Hz, 2H), 7.72 – 7.67 (m, 1H), 7.47 – 7.27 (m, 15H), 7.23 (dd, J = 11.7, 4.6 Hz, 2H), 6.92 (d, J = 0.5 Hz, 1H). **¹³C NMR** (101 MHz, $CDCl_3$) δ 172.31, 171.19, 142.50, 141.87, 141.43, 141.18, 137.70, 136.84, 135.94, 135.33, 132.79, 132.40, 130.17 (s), 129.76, 128.76, 128.51, 128.25, 127.09, 125.15, 124.70, 124.14, 123.89, 119.56, 118.81, 118.22, 111.42, 109.20, 88.65, 77.50, 76.97, 76.69. **HRMS** m/z: 640.72 [M+H]⁺.

5,7-Bis(2-(4,6-diphenyl-1,3,5-triazin-2-yl)phenyl)-5,7-dihydroindolo[2,3-b]carbazole (BBCz-o-2TRZ)

2-(2-Fluorophenyl)-4,6-diphenyl-1,3,5-triazine (FTRZ) (1.66 g, 5.06 mmol), 5,7-dihydroindolo[2,3-b]carbazole (0.59 g, 2.3 mmol), Cs_2CO_3 (2.99 g, 9.2 mmol) were added to a 100 ml three-necked flask under argon protection. After the mixture was degassed with argon for 3 times, anhydrous DMF solution (60 mL) was added, and then the mixture was heated to reflux for 24 hours. The reaction was quenched by H_2O. The reaction mixture was cooled to room temperature and extracted with dichloromethane. After the solvent evaporated under a reduced pressure, the residue was purified by column chromatography (DCM/PE=1/50) to afford **BBCz-o-2TRZ**

(1.3 g, 65%). **¹H NMR** (400 MHz, CDCl₃) δ 8.53 (s, 1H), 8.40 (dd, J = 7.8, 1.4 Hz, 2H), 8.08 – 8.04 (m, 2H), 8.02 – 7.95 (m, 8H), 7.62 (td, J = 7.7, 1.1 Hz, 2H), 7.47 – 7.41 (m, 6H), 7.36 – 7.32 (m, 2H), 7.27 (d, J = 8.2 Hz, 6H), 7.22 (ddd, J = 8.3, 6.1, 1.7 Hz, 6H), 7.13 (d, J = 7.4 Hz, 2H), 6.78 (s, 1H). **¹³C NMR** (101 MHz, CDCl₃) δ 172.26, 171.19, 142.23, 142.00, 136.75, 135.69, 135.42, 132.80 , 130.30, 128.80, 128.33, 124.87, 124.16, 119.41, 118.55, 111.41, 109.03, 88.59, 77.30, 77.03, 76.72. **HRMS** m/z: 871.37 [M+H]⁺.
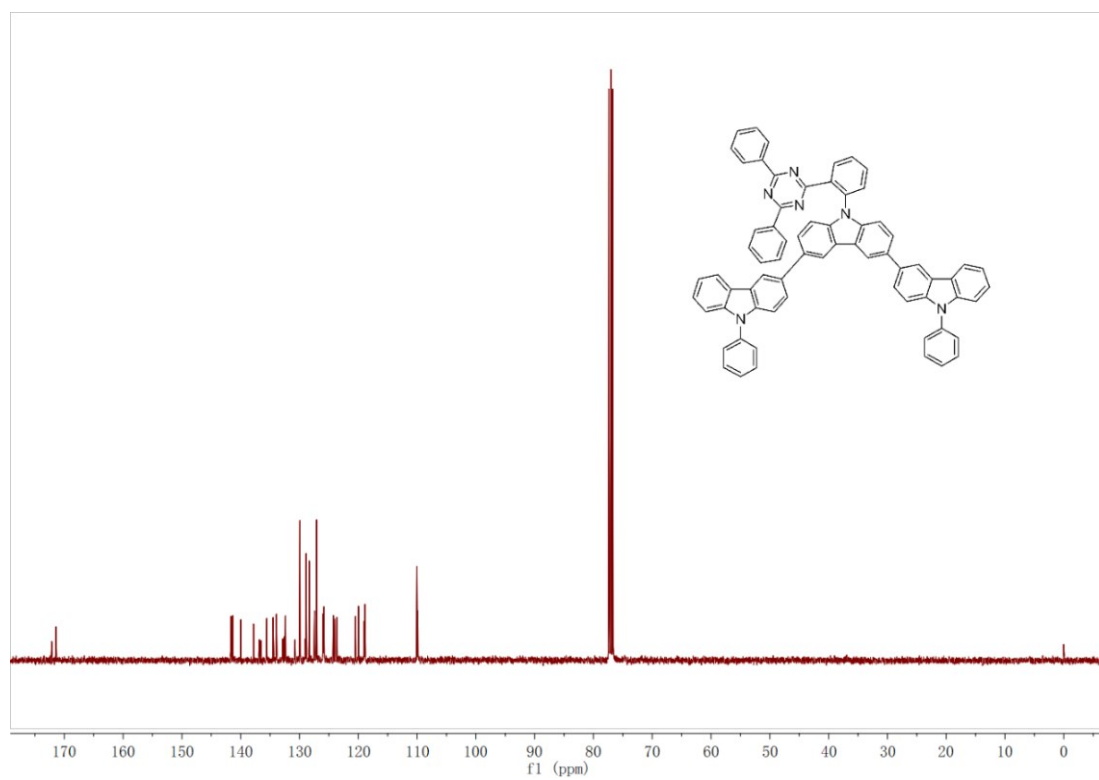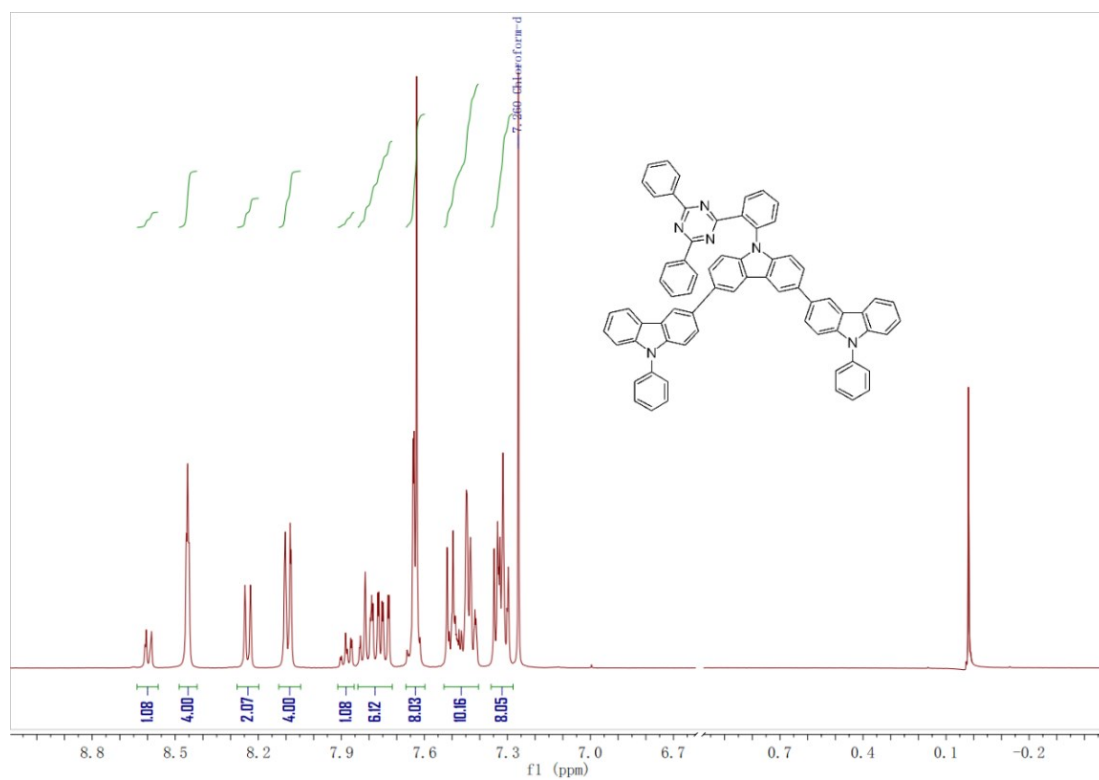
Figure S15. ^{1}H NMR and ^{13}C NMR spectra of TCz-o-TRZ.
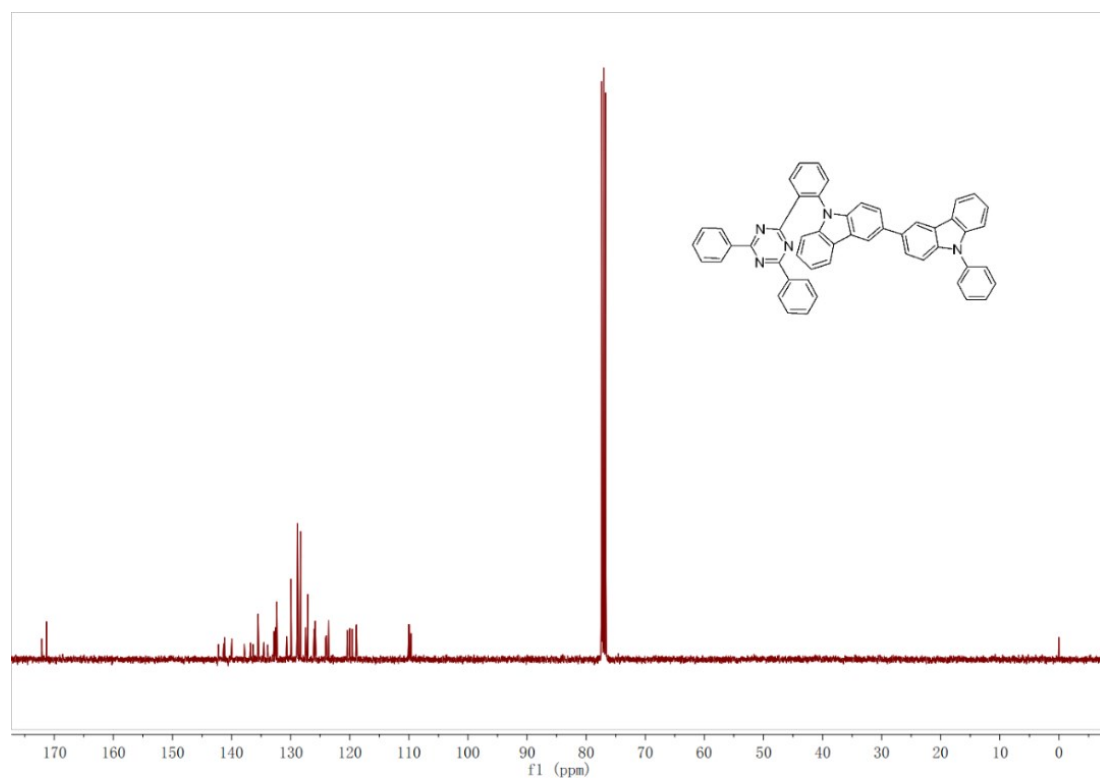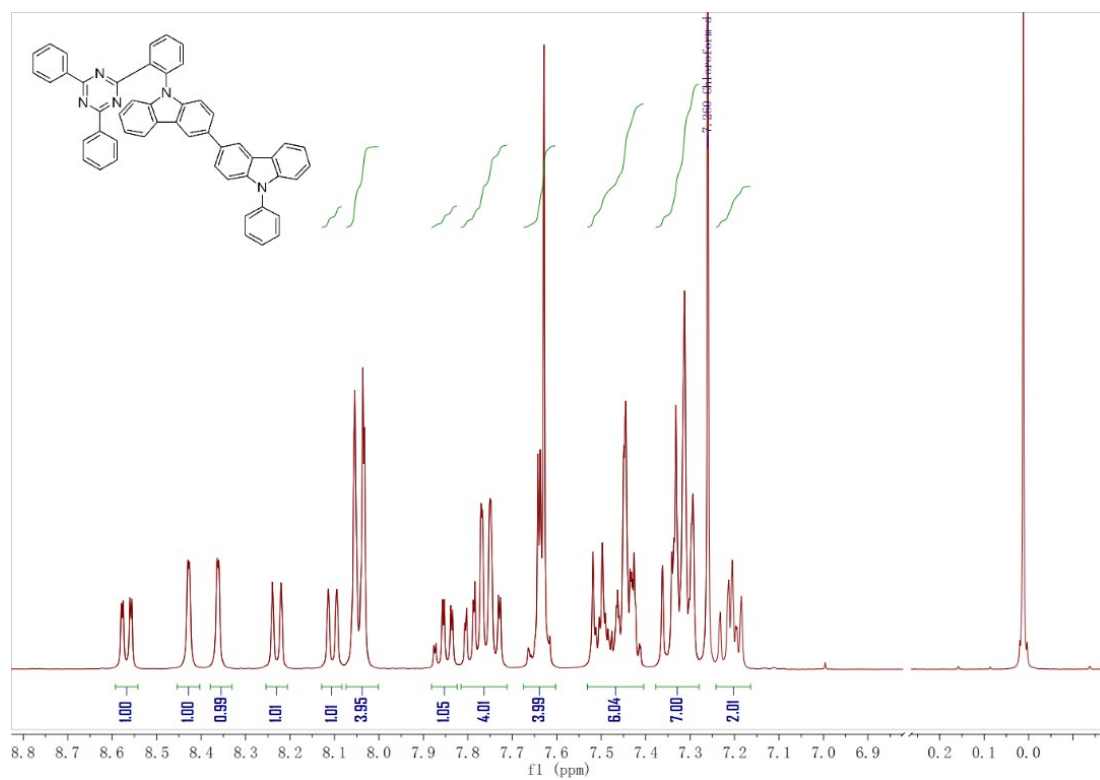
Figure S16. ^{1}H NMR and ^{13}C NMR spectra of BCz-o-TRZ.
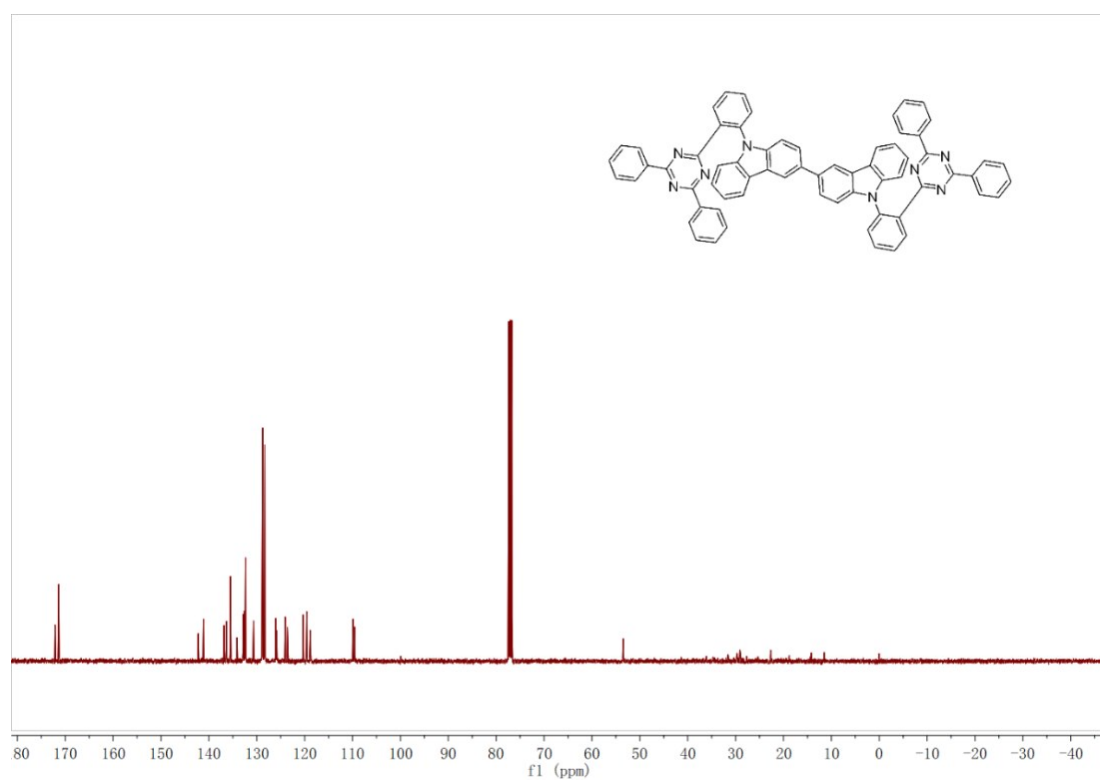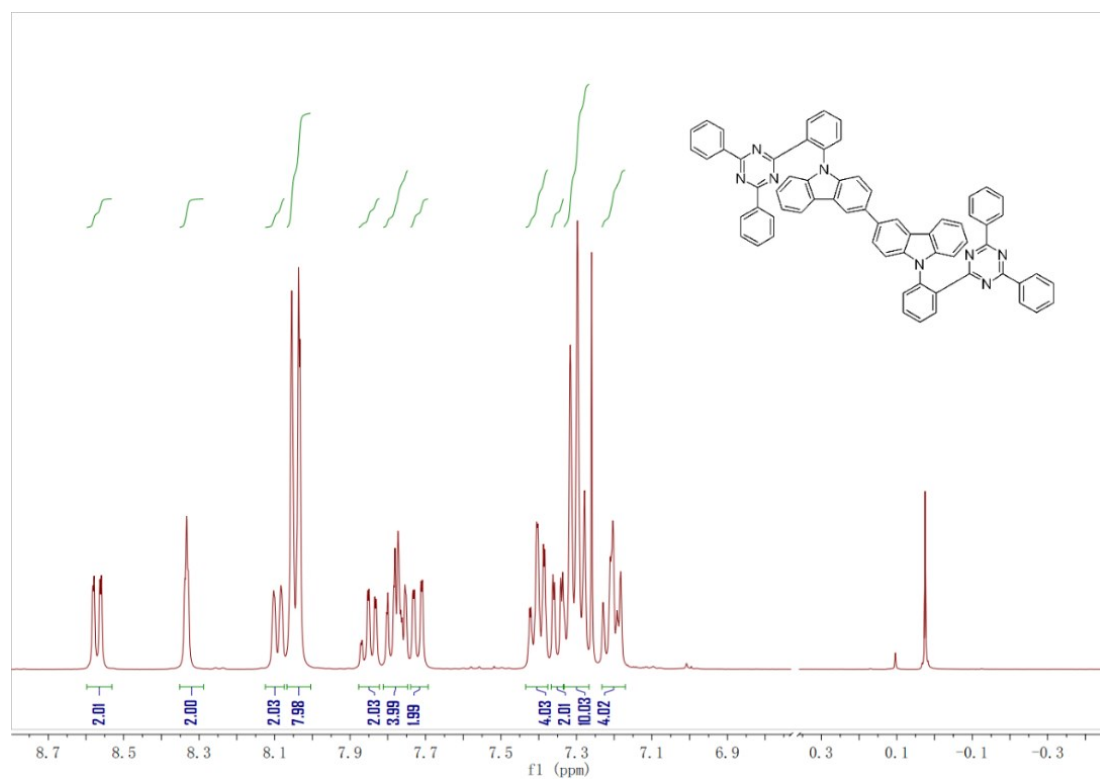
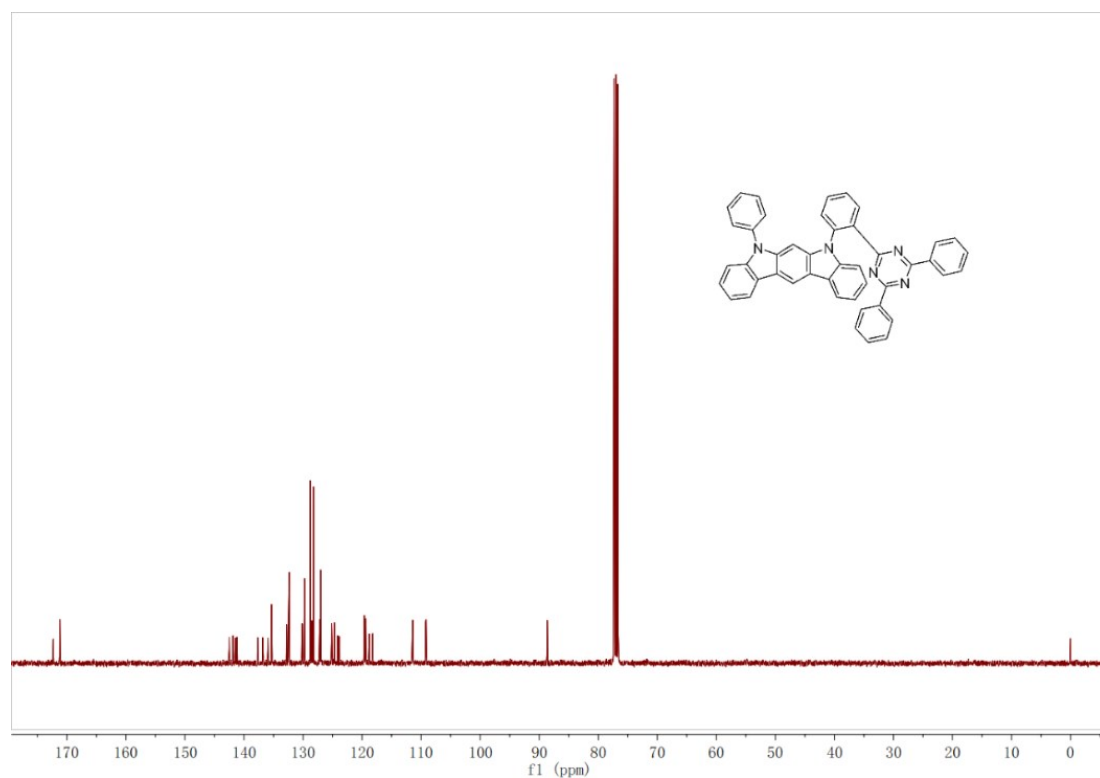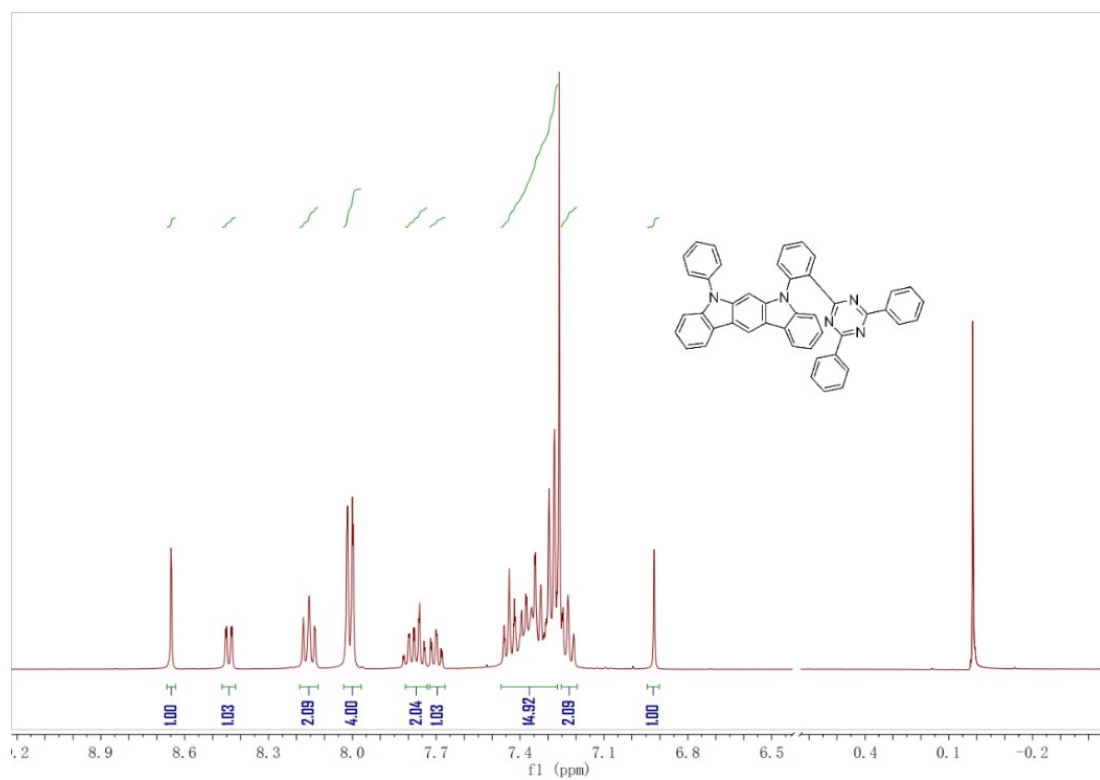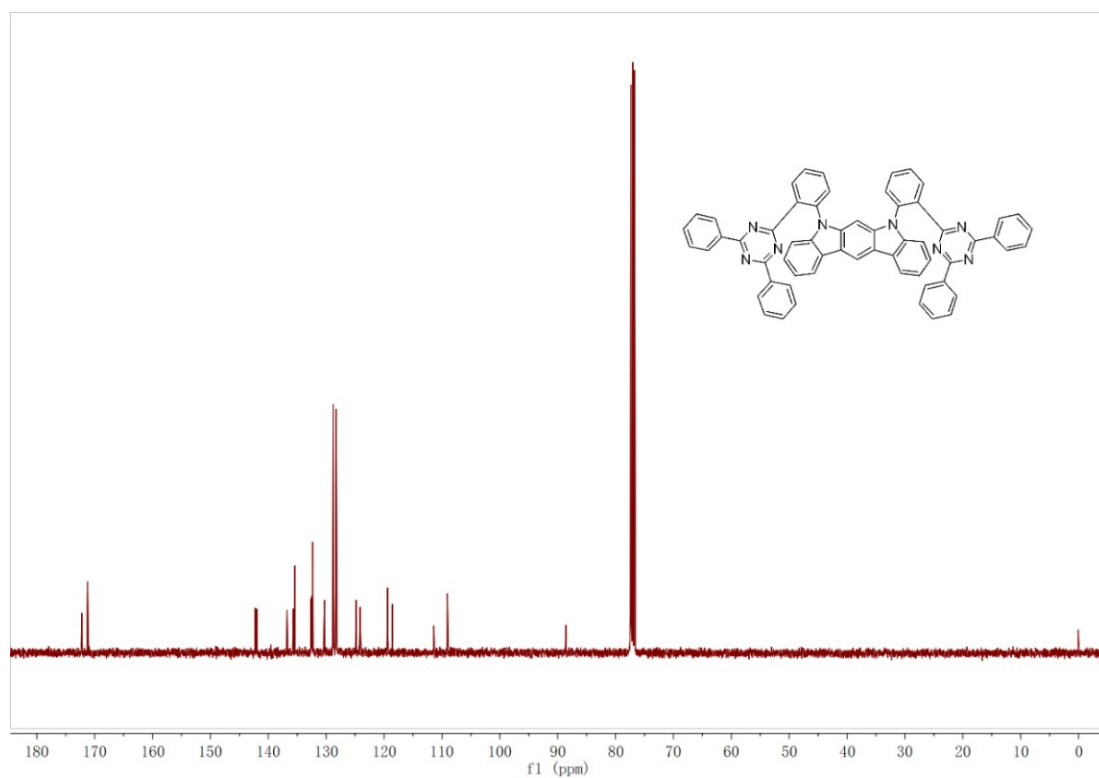**Figure S17.** ^{1}H NMR and ^{13}C NMR spectra of BCz-o-2TRZ.

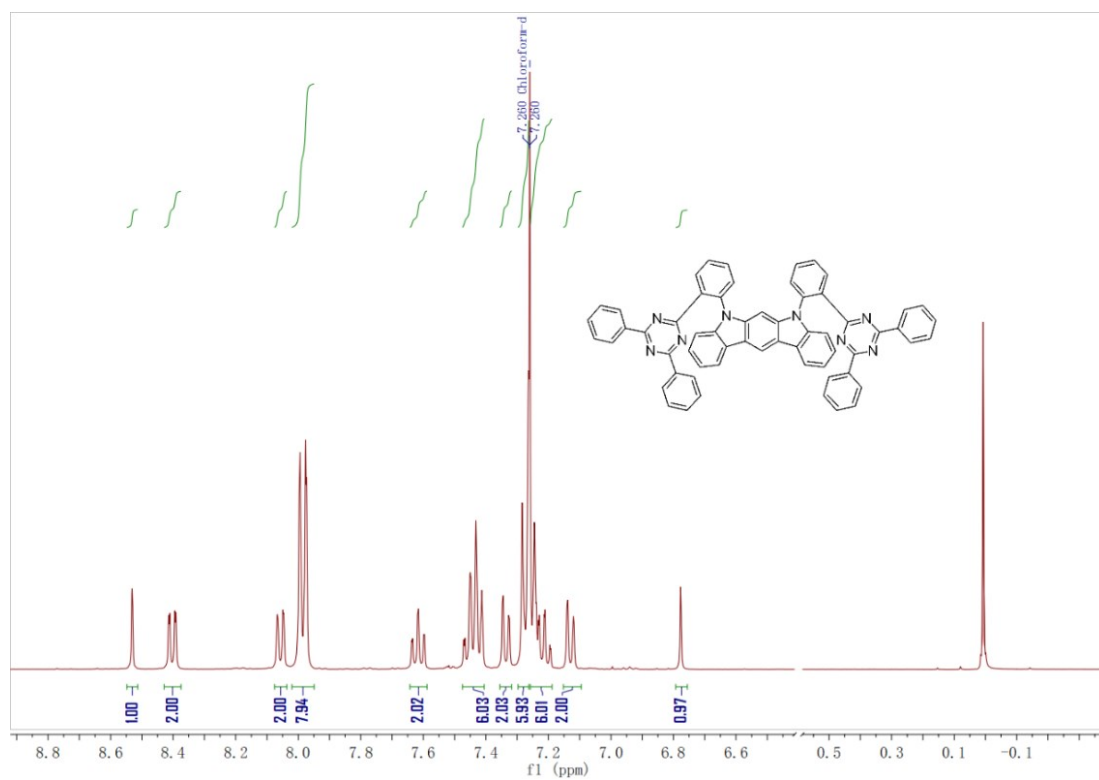**Figure S18.** ^{1}H NMR and ^{13}C NMR spectra of BBCz-o-TRZ.

Figure S19. ^{1}H NMR and ^{13}C NMR spectra of BBCz-o-2TRZ.

2.3 Photoluminescence measurements:

The absorption and emission spectra were recorded using a Shimadzu UV-2600 spectrophotometer and a PTI QM-40 spectrofluorometer, respectively. The photoluminescence quantum yields (PLQYs) of the samples were measured using the PTI spectrofluorometer equipped with an integrating sphere. The low-temperature fluorescence (1 ns) and phosphorescence (100−1000 μs) spectra were collected by the PTI spectrofluorometer employing the strobe technique and an electric shutter, respectively. The excitation source is a nitrogen laser (GL-3300, λ=266 nm, pulse width ∼1 ns, pulse energy=1.45 mJ). The transient PL decay spectra were recorded on a Horiba DeltaFlex modular lifetime measurement system patented TCSPC technique.

2.4 Electrochemical measurements:

Cyclic voltammetry were performed using a CHI 600E electrochemical analyzer in a gas-tight three-electrode cell at room temperature. A glassy carbon working electrode (Φ = 5.0 mm), a platinum wire auxiliary electrode, and an Ag/Ag^+ reference electrodes (0.1 M $AgNO_3$, 0.1 M tetrabutylammonium hexafluorophosphate in acetonitrile) were used. The reduction processes were measured by scanning the potential at a scan rate of 100 mV/s in acetonitrile, with 0.1 M tetrabutylammonium hexafluorophosphate (TBAP) as supporting electrolyte. The solutions were degassed by purging with N_2 gas for approximately 3 minutes before the measurement. The ferrocene couple Fc^+/Fc was selected as the external reference.

2.5 Quantum chemical calculations:

All calculations were performed using the Gaussian 09 program package.[4] The geometries in the ground state were optimized via DFT calculations at the B3LYP/6-31G* level in vacuum. Frequency analysis was used to confirm that the structures are at the local minima of the potential surfaces. Vertical absorption energies (E_{VA}) were calculated based on TDDFT with the B3LYP, PBE0, MPW1B95, BMK, M06-2X and M06-HF functionals using 6-31G* basis sets in vacuum. The zero-zero energies (E_{0-0}) were calculated by a previously reported OHF-q method.[3] The details on the

calculations of CT amount (q), optimal HF%, $E_{0\text{-}0}(^1CT)$, $E_{0\text{-}0}(^3CT)$ and $E_{0\text{-}0}(^3LE)$ can be found in Table S1 and the previous report.[1] The mean localization distance of HOMO (R_{LOL}) were calculated at the LOL-tuned LC-ωPBE^{LOL}/Def2-SVP level based on the geometries optimized at the CAM- B3LYP/Def2-SVP level in toluene SMD solution.[5] These levels of theory have been proven reliably for the calculation of TADF emitters.[6] R_{LOL} was calculated using modified version of Multiwfn 3.4.0[2] and it is defined as below:[5]

$$R_{LOL} = \sqrt{\frac{\int LOL(r) r^2 LOL(r) dr}{\int LOL(r) LOL(r) dr}}$$

where LOL is the localized orbital locator, a relative index based on kinetic energy density for measuring the localization of electron density.[7]

2.6 Device fabrication and measurements:

After the pre-cleaned indium tin oxide (ITO) glass substrates had been treated with ultraviolet-ozone for 15 minutes, the inorganic, organic and metal layers were thermally evaporated onto the substrates in an inert chamber under a pressure of 2×10^{-4} Pa. The deposition rates were 0.1 Å/s for MoO_3, 1-2 Å/s for organic layers, and 4 Å/s for Al layer. The current density, voltage and luminance characteristics of the devices were measured in ambient air with a Keithey 2400 Source meter and a Keithey 2000 Source multimeter equipped with a calibrated silicon photodiode. The electroluminescence spectra were recorded using a multichannel spectrometer (PMA12, Hamamatsu Photonics). Assuming Lambertian emission, the external quantum efficiency can be calculated from the luminance, current density, and EL spectrum.

3. Photodegradation kinetics in the BBCz-o-TRZ film

Assuming that the coupling reaction (A+A→B) in the BBCz-o-TRZ doped film is essentially irreversible, the disappearance rate of A can be expressed using a differential rate equation:

$$-\frac{d[A]}{dt} = k[A]^2 \qquad (1)$$

where [A] is the concentration of A, and k is the reaction rate constant. Rearranging equation 1 and integrating it leads to:

$$\frac{1}{[A]_t} = kt + \frac{1}{[A]_0} \qquad (2)$$

For a second order reaction with unique reactant, a linear relationship between $\frac{1}{[A]_t}$ and time can be expected:
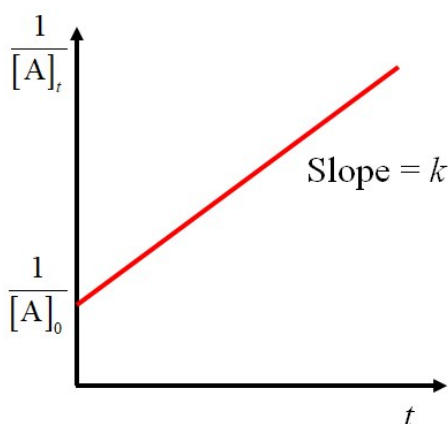

Figure S20. Linear relationship between the inverse of reactant concentration and the reaction time.

For the photodegradation process in BBCz-o-2TRZ doped films, the reactant is BBCz-o-2TRZ. The PL intensity of the doped film is inversely proportional to the concentration of the reaction product, which performs as the quenching center in the film. Consequently, the [PL intensity] of the doped film is deduced to be proportional to [A]. The 1/[PL intensity] of BBCz-o-2TRZ versus time is plotted in Figure S18. The linear relationship between 1/[PL intensity] and time indicates a second-order reaction in the BBCz-o-2TRZ doped thin film under UV irradiation. According to Figure S18, the reaction rate concentration k and $[A]_0$ is calculated to be 2.58×10^{-4}

a.u.$^{-1}$min^{-1} and 558.66 a.u., respectively. Employing these two parameters, a theoretical curve is presented in Figure S19, which fits well with the experimental PL decay curve.
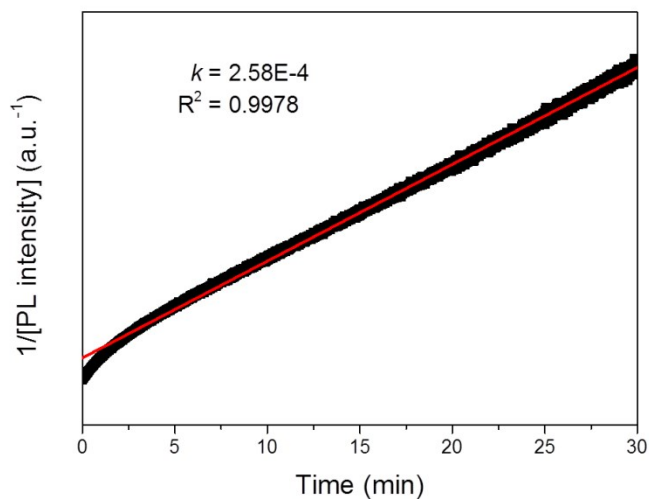
Figure S21. Plot of 1/[BBCz-o-2TRZ] versus time.
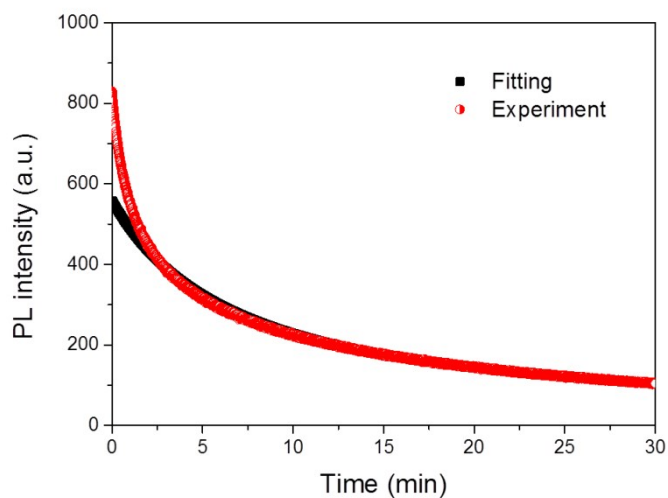
Figure S22. Photoluminescence decay of BBCz-o-2TRZ doped into a PYD2 film (30 wt%), which can be well fitted according to a second-order reaction kinetics.

4. References

(1) Zhang, Q.; Li, B.; Huang, S.; Nomura, H.; Tanaka, H.; Adachi, C. Efficient blue organic light-emitting diodes employing thermally activated delayed fluorescence. *Nat. Photonics* **2014**, *8*, 326–332.

(2) Lu, T.; Chen, F. Multiwfn: A Multifunctional Wavefunction Analyzer. *J. Comp. Chem.* **2012**, *33*, 580−592.

(3) Huang, S.; Zhang, Q.; Shiota, Y.; Nakagawa, T.; Kuwabara, K.; Yoshizawa, K.; Adachi, C. Computational Prediction for Singlet- and Triplet-Transition Energies of Charge-Transfer Compounds *J. Chem. Theory Comput.* **2013**, *9*, 3872−3877.

(4) Frisch, M. J.; Trucks, G. W.; Schlegel, H. B.; Scuseria, G. E.; Robb, M. A.; Cheeseman, J. R.; Scalmani, G.; Barone, V.; Mennucci, B.; Petersson, G. A.; Nakatsuji, H.; Caricato, M.; Li, X.; Hratchian, H. P.; Izmaylov, A. F.; Bloino, J.; Zheng, G.; Sonnenberg, J. L.; Hada, M.; Ehara, M.; Toyota, K.; Fukuda, R.; Hasegawa, J.; Ishida, M.; Nakajima, T.; Honda, Y.; Kitao, O.; Nakai, H.; Vreven, T.; Montgomery, Jr., J. A.; Peralta, J. E.; Ogliaro, F.; Bearpark, M.; Heyd, J. J.; Brothers, E.; Kudin, K. N.; Staroverov, V. N.; Keith, T.; Kobayashi, R.; Normand, J.; Raghavachari, K.; Rendell, A.; Burant, J. C.; Iyengar, S. S.; Tomasi, J.; Cossi, M.; Rega, N.; Millam, J. M.; Klene, M.; Knox, J. E.; Cross, J. B.; Bakken, V.; Adamo, C.; Jaramillo, J.; Gomperts, R.; Stratmann, R. E.; Yazyev, O.; Austin, A. J.; Cammi, R.; Pomelli, C.; Ochterski, J. W.; Martin, R. L.; Morokuma, K.; Zakrzewski, V. G.; Voth, G. A.; Salvador, P.; Dannenberg, J. J.; Dapprich, S.; Daniels, A. D.; Farkas, O.; Foresman, J. B.; Ortiz, J. V.; Cioslowski, J.; Fox, D. J. Gaussion 09, Revision D.01; Gaussian, Inc.: 2009.

(5) Wang, C.; Zhang, Q. Understanding Solid-State Solvation-Enhanced Thermally Activated Delayed Fluorescence Using a Descriptor-Tuned Screened Range-Separated Functional. *J. Phys. Chem. C* **2019,** *123*, 4407−4416.

(6) Wang, C.; Zhou, K.; Huang, S.; Zhang, Q. Toward an Accurate Description of Thermally Activated Delayed Fluorescence: Equal Importance of Electronic and Geometric Factors. *J. Phys. Chem. C* **2019,** *123*, 13869−13876.

(7) Schmider, H. L.; Becke, A. D. Chemical content of the kinetic energy density. *J. Mol. Struct.: THEOCHEM* **2000,** *527*, 51−61.